Electronic Supplementary Information

Phase transition induced improvement in H_2 desorption kinetics: the case of the high-temperature form of $Y(BH_4)_3$.

Tomasz Jaroń [1], Wiktor Koźmiński [1], and Wojciech Grochala [1,2*]

[1] *Faculty of Chemistry, The University of Warsaw, Pasteura 1, 02093 Warsaw, Poland.*

[2] *ICM, The University of Warsaw, Pawińskiego 5a, 02106 Warsaw, Poland.*

* *e-mail: wg22@cornell.edu*

1. Methodology

All substrates were fine quality anhydrous chemicals from Sigma–Aldrich ($LiBH_4$ >95 %, YCl_3 >99.9 % on metal basis). To avoid hydrolysis all reactions were performed (and all samples were stored) in an inert gas (Ar) atmosphere of the MBRAUN Labmaster DP glovebox (<0.1 ppm O_2, <0.1 ppm H_2O).

Dry (mechanochemical) synthesis of $Y(BH_4)_3$. For mechanochemical synthesis the vibrating mill (Testchem) and chromium steel bowl and disc were used. Substrates, YCl_3 and $LiBH_4$ were mixed in ca 1:3 molar ratio (with a 5 % excess of MBH_4) and milled for *ca.* 60 minutes in Ar atmosphere. Milling periods of 3–5 minutes were altered with 2–5 minutes rests to avoid thermal decomposition of the products. Temperature of the milling bowl did not exceed 40 °C as measured by a pyrometer.

Thermal decomposition. Thermal decomposition of samples was investigated with a thermogravimeter (TGA) and differential scanning calorimeter (DSC) combined in a simultaneous thermal analyser STA 409 PG (Netzsch) at a constant Ar (99.999 %) flow of 50 or 70 ml/min. Simultaneously the evolved gases were analysed with a quadrupole mass spectrometer QMS 403 C (Pfeiffer Vacuum) and a vacuum infrared spectrometer Vertex 80v (Bruker). The spectrometers were connected to the TGA/DSC device by quartz capillary and Teflon® tube, respectively. Both transfer lines were preheated to 200 °C to avoid condensation of low-boiling volatiles. Samples were placed inside Al_2O_3 crucibles with alumina cover and were heated at various heating rates (1 or 10 K/min).

To quench high-temperature phase of $Y(BH_4)_3$ the samples were slowly heated to a specific temperature (at 1 K/min) and then rapidly cooled (at 40–50 K/min) via a liquid nitrogen cooling system of the TGA furnace.

Infrared spectroscopy. Infrared absorption spectra of all solid products were measured using Vertex 80v FT-IR spectrometer (Bruker). Anhydrous KBr was used as a pellet material.

X-ray diffraction. Solid products sealed inside the 1 mm or 0.3 mm quartz capillaries were investigated by X-ray powder diffraction using the D8 Discover diffractometer from Bruker (a parallel beam; the $CuK_{\alpha 1}$ and $CuK_{\alpha 2}$ intensity ratio of ca. 2:1).

X-ray diffraction analysis. Powder X-ray diffraction patterns (XRDPs) were processed in Materials Studio 4.2 from Accelrys. The X-Cell program [1] has been used for indexing and determination of systematic absences. Reflex program (Materials Studio suite) was used for structure refinement and solution.

NMR Spectroscopy. Magic Angle spinning (MAS) ^{1}H and Cross Polarisation CP/MAS ^{89}Y spectra were measured on Varian spectrometer with 16.4 T Oxford Instruments magnet. Zirconia 3.2 mm outer diameter rotors have been used with spinning rate of 15 – 20 kHz for ^{1}H, and 2 kHz for ^{89}Y. For ^{89}Y an acquisition time of 30 ms and a repetition delay of 3 s was applied for 717 – 1000 independent scans with ^{1}H decoupling. $YCl_3 \cdot 6H_2O$ has been used as ^{89}Y chemical shift standard, δ = 58 ppm *vs.* 1 mol/dm^3 water solution of YCl_3 [2,3].

DFT Calculations. DFT calculations (energy, atom position relaxation and phonon dispersion) have been performed in VASP [4] and Phonon [5] programs included in MedeA package. The calculations were performed using GGA method with the PBE correlation-exchange functional and ultrasoft Vanderbildt-type pseudopotentials. We have used the 600 eV cut off and the k-point grid of *ca.* 0.11 Å^{-1}. The electronic iterations convergence was 10^{-6} eV per atom for geometry optimisation and 10^{-7} eV per atom for phonon calculations.

2. XRD powder pattern and structure solution

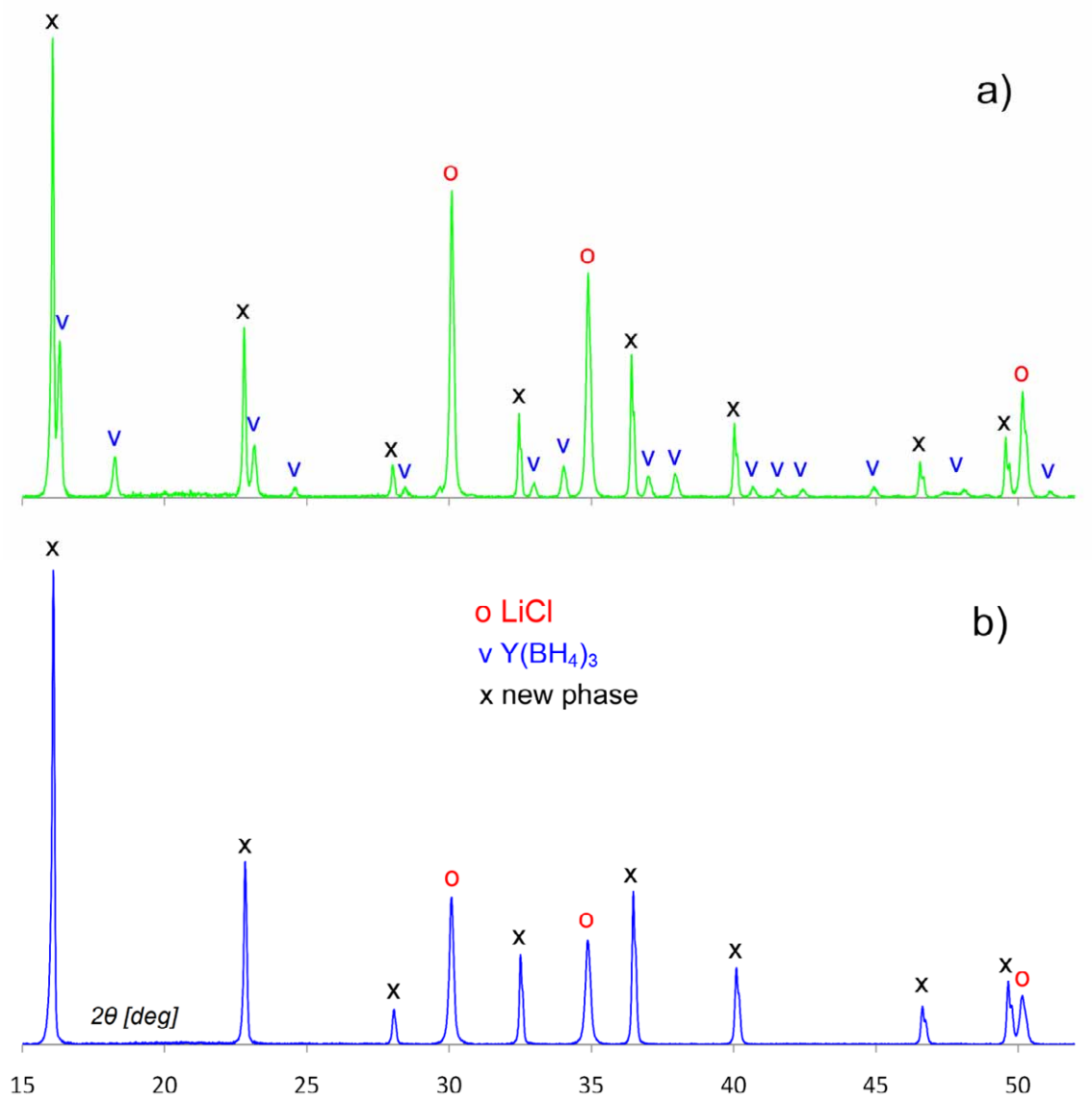

Fig. S1. X-ray powder pattern of a) $Y(BH_4)_3$ + 3 LiCl heated to 210 °C at 1 K/min, b) $Y(BD_4)_3$ + 3 LiCl heated to 216 °C at 1 K/min, both samples quenched fast to room temperature. The background has been removed for clarity.

The X-ray diffraction pattern of the HT-$Y(BH_4)_3$ sample shows very strong reflexes from this phase together with much weaker ones from the low-temperature phase of $Y(BH_4)_3$, still present in the sample at 195–210 °C. In the samples heated to a slightly higher temperature (216 °C for $Y(BD_4)_3$), only the new phase and LiCl could be detected by X-ray powder diffraction. Importantly, the X-ray powder patterns of products obtained by heating to temperatures exceeding 229 °C showed only reflexes from LiCl, suggesting that amorphization and/or thermal decomposition takes place. Reflexes from the HT phase of $Y(BH_4)_3$ have been successfully indexed with X-Cell. The best solutions were cubic, a = 5.512 Å (V = 167.5 $Å^3$) and 11.024 Å (V = 1340 $Å^3$), with extinction classes of P23 and F–43c, respectively. The volume of the P23 unit cell (167.5

Å^3, identical to 1/8 V of the F–43c unit cell) is only 4.8 % larger than the molar volume of the low–temperature phase of $Y(BH_4)_3$ (159.8 Å^3). According to this observation and only a minor mass loss accompanying the phase transformation (*ca.* 0.4 wt. %), the new phase may be safely assumed to be a high-temperature polymorph of $Y(BH_4)_3$ (metastable at ambient conditions). Space group search in X-Cell led to several solutions, among which P23, P-43m (a = 5.512 Å) and F23, F-43m, Ia-3 (a = 11.024 Å) were considered as six starting models of the unit cell of HT-$Y(BH_4)_3$ (there were two different models of Ia-3 symmetry). In the meantime, works by Ravnsbæk *et al.* and Frommen *et al.* have appeared in press, the latter one suggesting the Fm-3c structure.

Due to inherent difficulties in structure solution of borohydrides from X-ray data (light hydrogen is in the neighbourhood of a heavy yttrium atom) we have supported our models of HT-$Y(BH_4)_3$ by periodic density functional theory calculations performed in VASP. We have relaxed atoms in the unit cells, and calculated internal (electronic and internuclear) energies of every phase. According to the calculations, the phase of the lowest energy is reached by relaxation of the starting F23 cell. This unit cell, however, converges to its F-43c supergroup (symmetrization at 0.1 Å threshold), which upon subsequent optimisation leads to a higher-symmetry Fm-3c cell (symmetrization at 0.01 Å threshold), virtually identical to the experimental cell from Frommen *et al.* The DFT-predicted distances were: Y–H *ca.* 2.32 Å, B–H *ca.* 1.23 Å, Y–B *ca.* 2.76 Å. Importantly, the calculated phonon dispersion showed no imaginary phonon modes thus proving its dynamic stability (see *Fig. S3*).

After Pawley refinement the refined unit cell vectors were: a = 10.889 ± 0.079 Å for HT-$Y(BH_4)_3$, and 11.0054 ± 0.0047 Å for HT-$Y(BD_4)_3$. The unit cells and the coordination spheres of Y centre in both low- and high-temperature forms of $Y(BH_4)_3$, are shown in the *Fig. S2*.

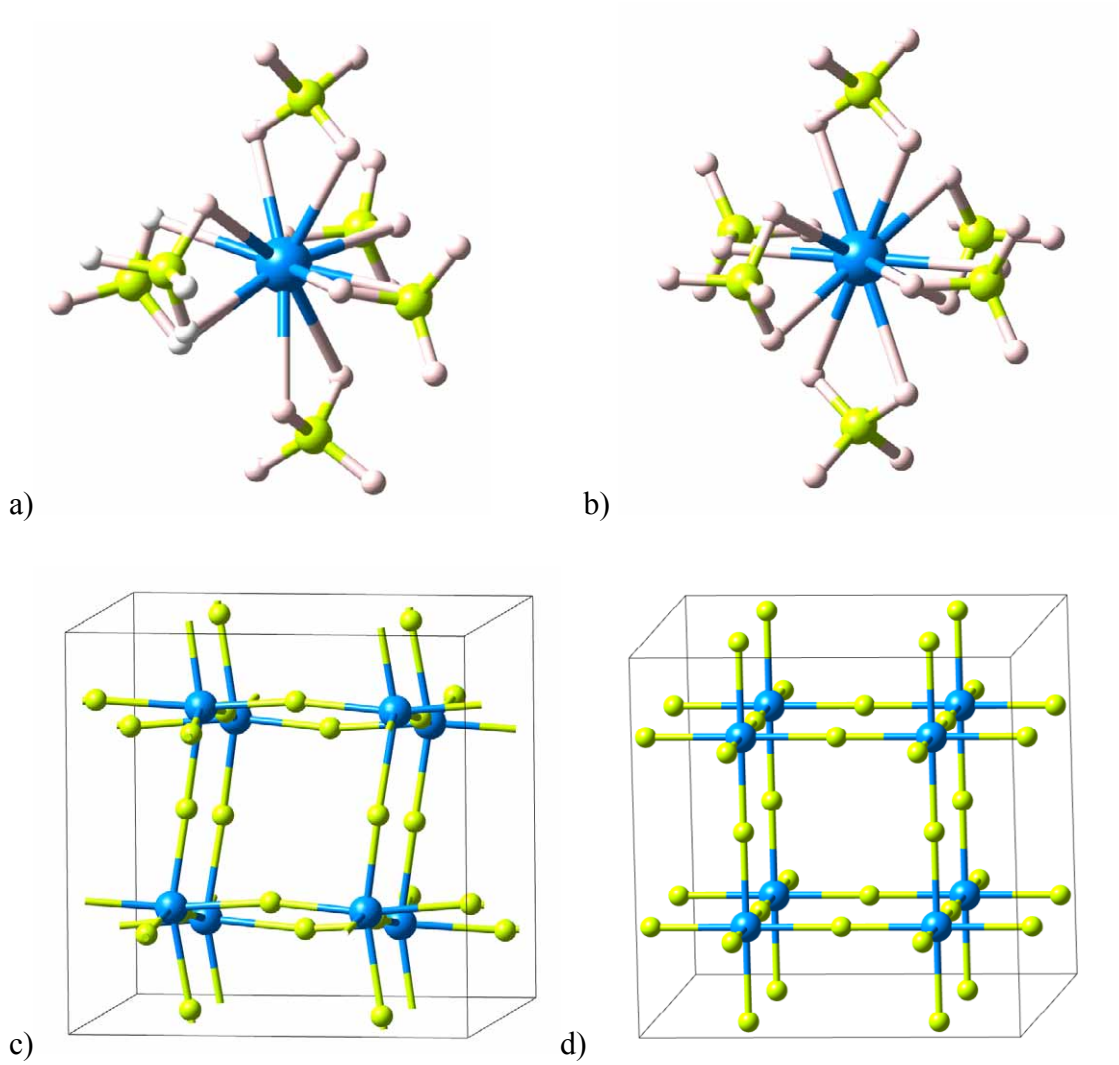

Fig. S2. a) Yttrium environment in LT-$Y(BH_4)_3$ [6], b) HT-$Y(BH_4)_3$ (this work), c) unit cell of LT-$Y(BH_4)_3$, d) unit cell of HT-$Y(BH_4)_3$, translated by (¼ ¼ ¼) from the original Fm-3c setting to show the relationship between the LT and HT cells. Hydrogen atoms have been removed for clarity in c) and d). Y – blue large balls, B – yellow medium balls, H – grey small balls.

3. Phonon Dispersion

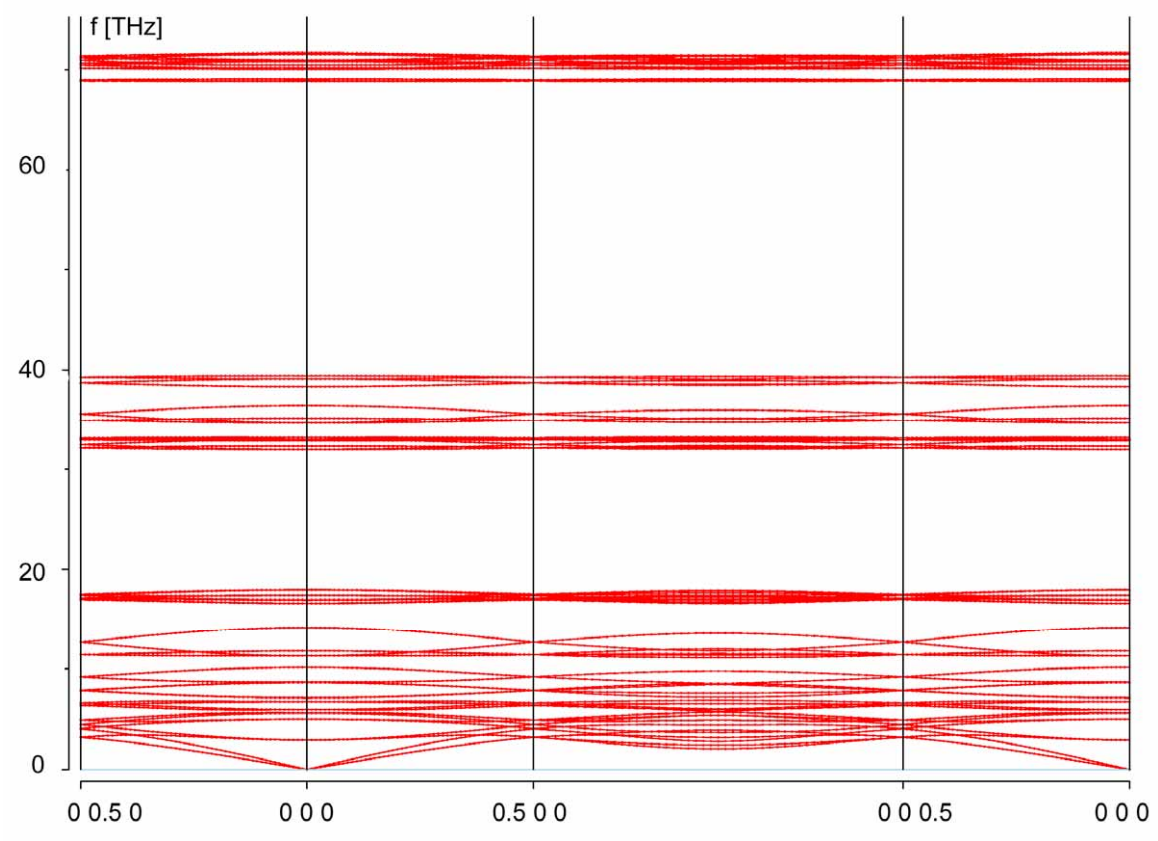

Fig. S3. Phonon dispersion plot of HT–$Y(BH_4)_3$. No imaginary phonon modes are present indicating dynamic stability of the unit cell.

4. NMR spectra

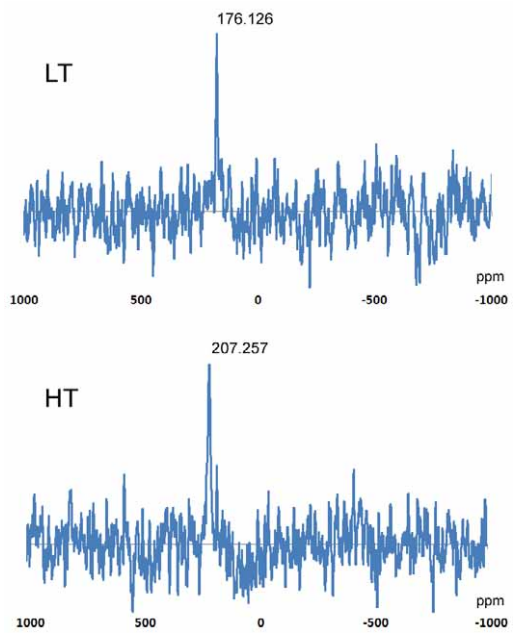

Fig. S4. ^{89}*Y CP MAS NMR spectra of LT(top) and HT (bottom) forms of* $Y(BH_4)_3$*. The values of* ^{89}*Y chemical shifts have been marked.*

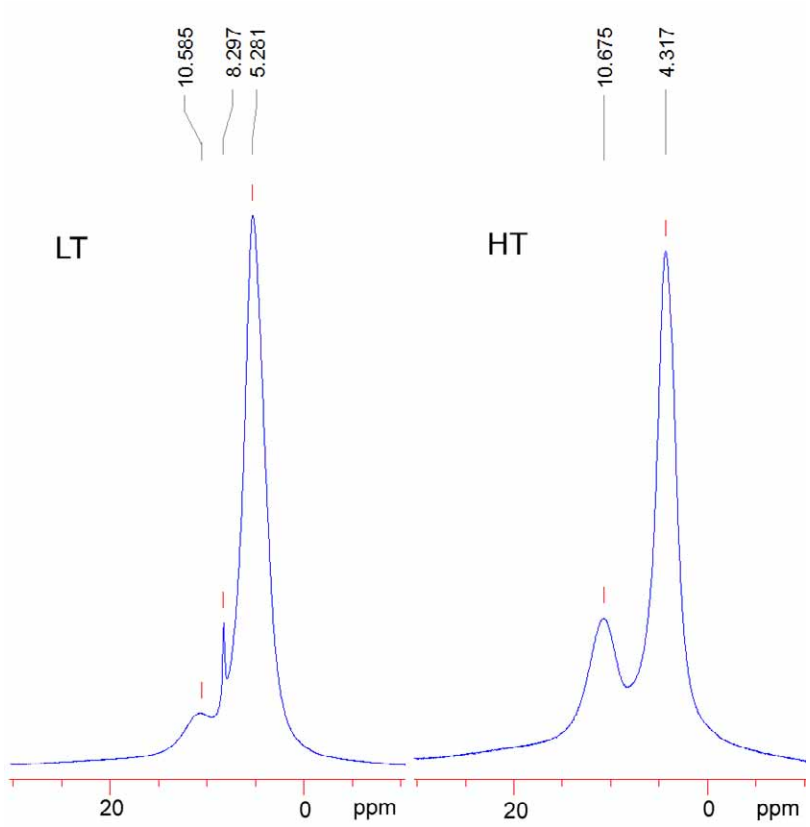

Fig. S5. ^{1}*H MAS NMR spectra of LT(left) and HT (right) forms of* $Y(BH_4)_3$*.*

$LiBH_4$ - in ^{1}H MAS NMR spectrum the borohydride peak occurs at −0.3 ppm[7].

$YCl_3 \cdot 6H_2O$ - ^{1}H MAS NMR signal at 9.91 ppm (this work).

5. ^1H NMR spin–lattice relaxation time

Spin–lattice relaxation time (T_1) of ^1H was measured with a common inversion–recovery method at 700 MHz (16.4 T). The temperature was stable usually within ±0.1 K error from the set value, except for the temperatures below 273 K, where the fluctuations up to ±1 K were noticed.

The values of the natural logarithms of relaxation rates (ln R_1) for both $Y(BH_4)_3$ polymorphs are plotted in *Fig. S6*, and listed in *Tab. S1*. The R_1 values of LT-$Y(BH_4)_3$ show an upward trend with increasing temperature, while the R_1 values of HT-$Y(BH_4)_3$ reveal a small minimum. However, in the latter case, the R_1 uncertainties are larger than the differences between the relaxation rate values and therefore, it is impossible to estimate the actual character of the R_1 vs. T^{-1} plot.

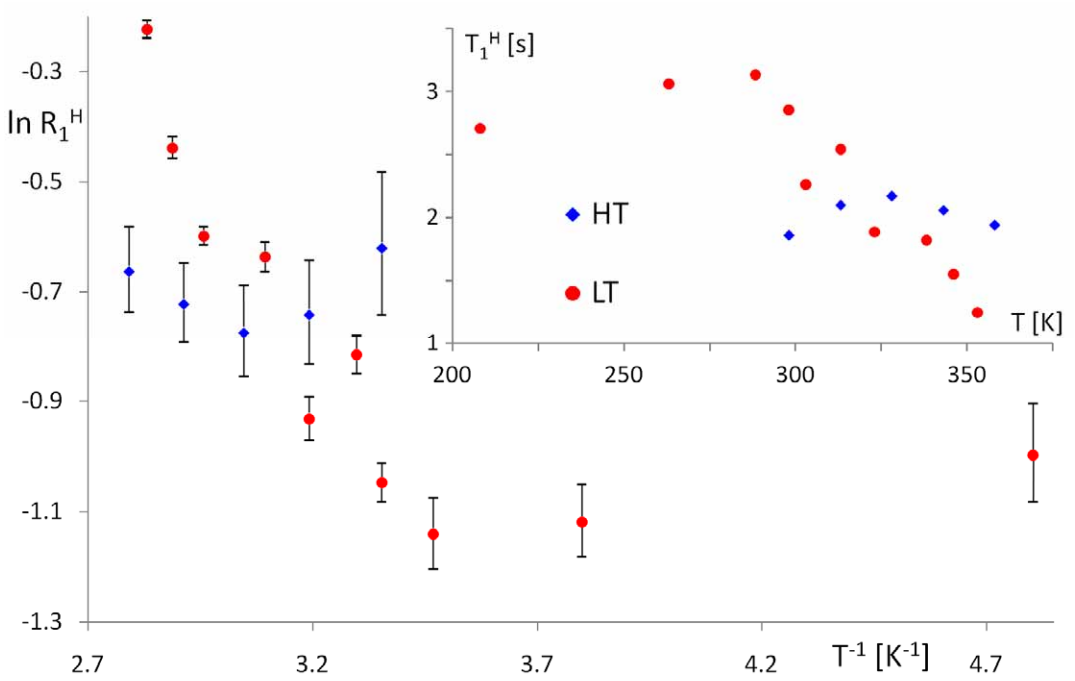

Fig. S6. Natural logarithm of the spin–lattice relaxation rates for LT and HT polymorphs of $Y(BH_4)_3$ versus the inverse of temperature. The errors of the fit of nuclear magnetisation recovery to a single exponential function has been marked. The insert: relaxation times (T_1) vs. temperature.

The rotations of BH_4^- anions in a few metal borohydrides have been previously investigated with NMR (*e.g.* $LiBH_4$ [8,9,10], $NaBH_4$ [8,11], KBH_4 [8,11], $Mg(BH_4)_2$ [12]). In such measurements, a maximum[13] in relaxation rate ($R_1 = T_1^{-1}$) is observed at the temperature at which the atomic jump rate, τ^{-1} (where τ, correlation time, represents the mean time between the hydrogen hoping) is close to the resonance frequency. The maximum divides the relaxation rate plot into two parts: a lower temperature "slow motion" region, and a higher temperature "fast motion" region. The Larmor's frequency of the protons in our experiment (700 MHz in spectrometer available to us) is one order of magnitude higher than frequencies typical for the borohydride motions (14–90 MHz), and

therefore no maxima have been observed in R_1 plots at the considered temperature range. Such a maximum is, however, expected at the temperature significantly higher than those covered by our measurements; unfortunately, thermal decomposition of $Y(BH_4)_3$ prevents such measurements.

Tab. S1. Results of the spin–lattice relaxation time measurements, together with errors of the fit of nuclear magnetisation recovery to a single exponential function.

polymorph	T [K]	T_1 [s]	δT_1 [s]
LT	208.15	2.71	0.24
	263.15	3.06	0.20
	288.25	3.13	0.20
	298.15	2.85	0.10
	303.15	2.26	0.08
	313.15	2.54	0.10
	323.15	1.89	0.05
	338.15	1.82	0.03
	346.15	1.55	0.03
	353.15	1.25	0.02
HT	298.15	1.86	0.26
	313.15	2.10	0.20
	328.15	2.17	0.18
	343.15	2.06	0.15
	358.15	1.94	0.15

The temperature dependence of τ^{-1} is often described by the Arrhenius equation:

$$\tau^{-1} = \tau_0^{-1} \exp(-E_A/RT) \quad (1)$$

According to this simple model, the plot of $\ln(R_1)$ *vs.* T^{-1} should be linear with a slope $\pm E_A/R$, taking positive sign for fast and negative one for slow motion region. We have attempted to fit the experimental data to the equation (1), while neglecting the two lowest temperature points for both LT and HT polymorphs, *Fig. S7*.

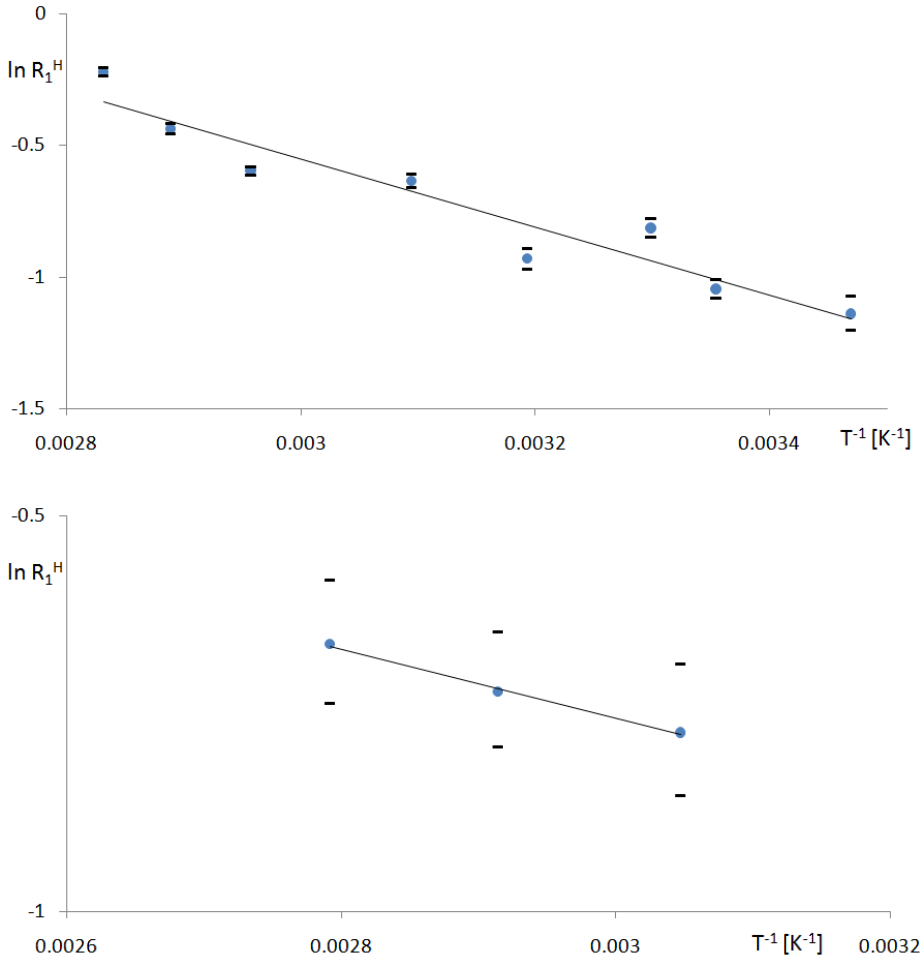

Fig. S7. The data fit to the Arrhenius equation. Top – LT polymorph, bottom– HT polymorph. The errors of the fit of nuclear magnetisation recovery to a single exponential function has been marked.

The calculated activation energy of BH_4^- motions is about three times higher for LT-$Y(BH_4)_3$ (E_A^{LT} = 11.3 kJ/mol, 120 meV), than for the HT form (E_A^{HT} = 3.6 kJ/mol, 37 meV). While the activation energy of BH_4^- rotations in LT-$Y(BH_4)_3$ is close to those observed for other borohydrides, the E_A of HT phase seems to be the smallest amongst these borohydrides for which such experimental data exist[12]. The latter result is, however, uncertain, due to small number of points taken to the fit and large errors in determination of T_1. It would be very interesting to repeat the T_1 measurements for the HT phase using a low-frequency NMR spectrometer.

6. Evaluation of kinetics of thermal decomposition using Urbanovici and Segal formalism

To examine $E_a(\alpha)$ over varying degrees of conversion we have performed TGA/DSC scans at heating rates of 5 and 10 K/min.

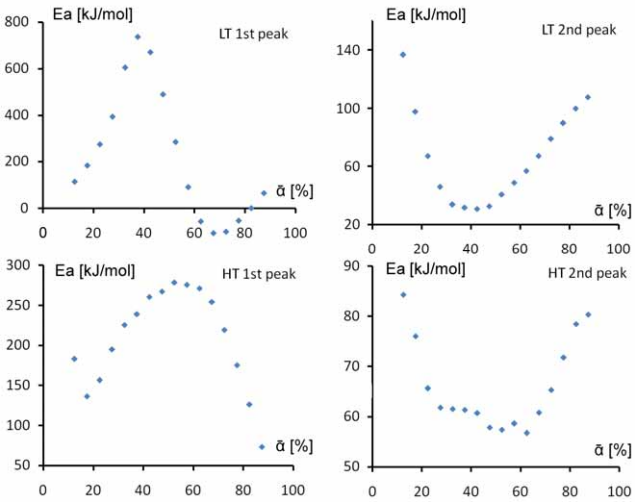

Fig. S8. Activation energy, E_a [kJ/mol], in function of conversion degree, α [%], according to Urbanovici and Segal (equation 3 in the main paper).

The activation energy changes with degree of conversion for both phases. The shape of the $E_a(\alpha)$ curves for the first DSC peak is different for both polymorphs, with a narrow maximum at 40% conversion degree for the LT phase[14] and a broad maximum at 60% conversion degree for the HT phase. The maximum value of $E_a(\alpha)$ agrees only roughly (with an error of up to 25 %) with the corresponding value of the activation energy according to Kissinger (Eq. 2 and *Table 2* in main paper). The shape of the $E_a(\alpha)$ curves of the second DSC peak is somewhat similar for both polymorphs. In brief, the results obtained according to formalism by Urbanovici and Segal confirm only qualitatively findings according to a simplistic Kissinger's approach.

7. References

[1] M. Neumann, *J. Appl. Cryst.*, **36** (2003) 356.

[2] A. R. Thompson, and E. Oldfield, *J. Chem. Soc., Chem. Commun.*, (1987) 27.

[3] J. Wu, T. J. Boyle, J. L. Shreeve, J. W. Ziller, and W. J. Evans, *Inorg. Chem.*, **32** (1993) 1130.

[4] G. Kresse and J. Furthmüller, *Phys. Rev. B*, **54** (1996) 11169.

[5] K. Parlinski, Software Phonon Cracow 2007 http://wolf.ifj.edu.pl/phonon/

[6] T. Sato, K. Miwa, Y. Nakamori, K. Ohoyama, H. W. Li, T. Noritake, M. Aoki, S. Towata and S. Orimo, *Phys. Rev. B*, **77** (2008) 104114.

[7] M. R. Hartman, J. J. Rush, T. J. Udovic, R. C. Bowman Jr., and S-J Hwang, *J. Solid State Chem.*, **180** (2007) 1298.

[8] T. Tsang, and T. C. Farrar, *J. Chem. Phys.*, **50** (1969) 3498.

[9] R. L. Corey, D. T. Shane, R. C. Bowman, Jr., and M. C. Conradi, *J. Phys. Chem. C*, **112** (2008) 18706.

[10] A. V. Skripov, A. V. Solonin, Y. Filinchuk, and D. Chernyshov, *J. Phys. Chem. C*, **112** (2008) 18701.

[11] O. A. Babanova, A. V. Solonin, A. P. Stepanov, A. V. Skripov, and Y. Filinchuk, *J. Phys. Chem. C*, **114** (2010) 3712.

[12] A. V. Skripov, A. V. Solonin, O. A. Babanova, H. Hagemann, and Y. Filinchuk, *J. Phys. Chem. C*, **114** (2010) 12370.

[13] If there are non-negligible differences in activation energy of rotation around various symmetry axes, a few maxima could in principle be observed.

[14] The function $E_a(\alpha)$ for the first decomposition stage of the LT phase reaches values below zero. This artefact is probably caused by overlapping processes with different E_a, which leads to changes in the DSC signal and the conversion function with the change of heating rate. Therefore only the values of *apparent* activation energy are traced in this method.